

Contribution from the Department of Chemistry, University of Missouri—Rolla, Rolla, Missouri 65401, the Nuclear Physics Division, Atomic Energy Research Establishment, Harwell, Didcot, OX 11 0RA, England, and the Inorganic Chemistry Laboratory, Oxford University, Oxford, OX1 3QR, England

## A Mössbauer-Effect Study of the Electronic and Magnetic Properties of Voltaite, a Mixed-Valence Mineral

GARY J. LONG,\*<sup>1a,b</sup> GEOFFREY LONGWORTH,<sup>1b</sup> PETER DAY,\*<sup>1c</sup> and DAVID BEVERIDGE<sup>1c</sup>

Received May 2, 1979

The Mössbauer-effect spectrum of voltaite,  $K_2Fe^{II}_5Fe^{III}_3Al(SO_4)_{12} \cdot 18H_2O$ , exhibits four well-resolved lines between room temperature and 4.2 K. Two of these quadrupole-split lines are assigned to the iron(II) ion, which occupies the M(2) site having the  $FeO_4(H_2O)_2$  pseudooctahedral coordination geometry. The remaining two lines are assigned to the iron(III) ions, which occupy both the M(2) site and the M(1) site which has the  $FeO_6$  octahedral coordination geometry. The relative intensities of these lines are in excellent agreement with earlier site occupancy factors established by single-crystal X-ray determinations and have a ratio of Fe(II),M(2) to Fe(III),M(1) to Fe(III),M(2) of 5:2:1. At 1.3 K, the intensity of the two iron(III) lines decreases significantly. This decrease is probably associated with the onset of ferrimagnetic ordering in the voltaite, an ordering that is reported to occur below 1 K. The Mössbauer-effect spectra of the solid-state solutions of cadmium in voltaite,  $K_2Fe^{II}_x Cd^{II}_{5-x} Fe^{III}_3 Al(SO_4)_{12} \cdot 18H_2O$ , in which  $x$  varies from 0.19 to 3.10, also exhibit four lines, but the iron(II) lines exhibit reduced intensity. An analysis of these spectra indicates that the quadrupole interaction at the iron(II) site decreases slightly as the cadmium content increases. The cubic lattice parameter for these compounds increases linearly as the cadmium content increases. The all-cadmium voltaite,  $K_2Cd_5Fe^{III}_3Al(SO_4)_{12} \cdot 18H_2O$ , exhibits two iron(III) Mössbauer absorption lines and remains paramagnetic down to 1.3 K. In an external applied magnetic field this compound exhibits different internal hyperfine fields on the two crystallographically different iron(III) sites. The relative intensities of the magnetic components are consistent with paramagnetic behavior, but the components are considerably broadened. At 4.2 K the internal hyperfine field increases from 72 to 333 kOe for the M(2) site and from 207 to 489 kOe for the M(1) site in external fields ranging from 2 to 6 T. At 1.7 K the Fe(II),M(1) site is very close to saturation and exhibits an internal hyperfine field of 555 kOe in a 6-T applied field. The Fe(III),M(2) site displays a distribution of hyperfine fields. It is suggested that the line broadening and the behavior of the spectra as a function of applied field are due to a combination of relaxation effects and to the presence of a range of hyperfine fields at Fe(III),M(2) sites due to the random occupation of M(2) sites by either Cd(II) or Fe(III).

### Introduction

The mixed-valence mineral voltaite and its solid solutions containing cadmium provide an interesting material, which can be used to study the relationship between structure, magnetic properties, and the magnitude of intervalent charge transfer. In an earlier paper, Beveridge and Day<sup>2</sup> described the synthesis, characterization, and optical properties of voltaite,  $K_2Fe^{II}_5Fe^{III}_3Al(SO_4)_{12} \cdot 18H_2O$ , and its solid-state solutions containing cadmium,  $K_2Fe^{II}_x Cd^{II}_{5-x} Fe^{III}_3 Al(SO_4)_{12} \cdot 18H_2O$ . In the present paper, we extend their study to include the electronic and magnetic properties.

Voltaite is an appropriate material to study for several reasons. Its crystalline structure is cubic and has been accurately determined by Mereiter.<sup>3</sup> Gossner<sup>4</sup> has shown that it can be used to form homogeneously substituted solid-state solutions in which a range of cations replace either the divalent or trivalent iron. The presence of iron in two different oxidation states and in crystallographically distinguishable sites<sup>3</sup> and the existence of an intervalence charge-transfer band<sup>2</sup> indicate that the mineral could be considered a class II type mixed-valency compound in the Robin and Day scheme.<sup>5</sup> Hence, one should be able to use the Mössbauer effect to determine the degree of difference in the electronic properties of a specific iron site from those found in a univalent compound of similar local symmetry and spin state. In voltaite, these properties can be studied as a function of mixed-valency interaction if one isomorphously substitutes one of the iron sites.

During the course of our investigation, Hermon et al.<sup>6</sup> published a Mössbauer and magnetic study of several voltaites. Our work extends upon their Mössbauer-effect studies and, in certain instances, differs from their work.

### Experimental Procedures

A method similar to that of Gossner and Arm<sup>7</sup> was employed to prepare samples of voltaite and its solid-state solutions containing

Table I. Analytical Results and Molecular Formula

Cd:Fe <sup>II</sup> prep ratio	x	x	% Fe		% Cd		Fe <sup>II</sup> : Fe <sup>III</sup> ratio	color
			calcd	obsd	calcd	obsd		
0:1	5.00	5.00	22.02	22.00			1.667	black
0.5:1	3.33	3.10	15.94	15.94	9.99	9.68	1.033	black
1:1	2.50	2.10	12.98	12.91	14.86	14.54	0.700	black
2:1	1.67	1.05	10.04	10.02	19.71	19.29	0.350	dark green
10:1	0.46	0.53	8.63	8.64	22.01	21.77	0.177	dark green
20:1	0.24	0.24	7.87	7.87	23.28	23.76	0.080	green
50:1	0.10	0.19	7.74	7.75	23.49	23.24	0.063	light green
Cd only	0	0	7.24	7.86	23.60	24.31	0	pale yellow

cadmium. The specific details of this preparative technique have been described by Beveridge and Day,<sup>2</sup> whose analytic studies include an atomic absorption analysis of the total iron and cadmium present and a volumetric analysis of the total iron and iron(II) present. The calculated and observed analytical results for the pure iron voltaite,  $K_2Fe^{II}_5Fe^{III}_3Al(SO_4)_{12} \cdot 18H_2O$ , agree closely, but the formulas for the cadmium-substituted voltaites,  $K_2Fe^{II}_x Cd^{II}_{5-x} Fe^{III}_3 Al(SO_4)_{12} \cdot 18H_2O$ , are not in agreement with the formula that one would expect from the ratio of cadmium to iron used in the preparation. Consequently, the value of  $x$  has been adjusted to yield as close an agreement as possible for the observed and calculated values of the iron and cadmium. The cadmium to iron preparative ratio, the optimum values

- (1) (a) Department of Chemistry, University of Missouri—Rolla. (b) Atomic Energy Research Establishment, Harwell. (c) Inorganic Chemistry Laboratory, Oxford University.
- (2) Beveridge, D.; Day, P. *J. Chem. Soc., Dalton Trans.*, 1979, 648.
- (3) Mereiter, K. *Tschermak's Mineral. Petrogr. Mitt.* 1972, 18, 185.
- (4) Gossner, B.; Drexler, K. *Zentralbl. Mineral. Geol. Palaeontol., Abst. A* 1933, 83.
- (5) Robin, M. B.; Day, P. *Adv. Inorg. Chem. Radiochem.* 1967, 10, 247.
- (6) Hermon, E.; Haddad, R.; Simkin, D.; Brandao, D. E.; Muir, W. B. *Can. J. Phys.* 1976, 54, 1149.
- (7) Gossner, B.; Arm, M. *Z. Kristallogr., Kristallgeom., Kristallphys., Kristallchem.*, 1929, 72, 202.

\* To whom correspondence should be addressed at the University of Missouri—Rolla or Oxford University.

**Table II.** Voltaite Crystal Structure<sup>a</sup>

stoichiometry	$K_2Fe_8Al(SO_4)_{12} \cdot 18H_2O$		
cryst syst	cubic		
space group	$Fd\bar{3}c, O_h^5$		
lattice parameter	27.254 (8)		
	27.249 (2) Å <sup>b</sup>		
<i>V</i>	20 244 Å <sup>3</sup>		
	20 233 Å <sup>3</sup> b		
<i>Z</i>	16		
<i>R</i>	0.033		
site designatn	M(1)	M(2)	total
symmetry	$\bar{3}$	2	
no./unit cell	32	96	128
Fe(III) occupancy	32	16	48
Fe(II) occupancy	0	80	80
coordin sphere	FeO <sub>6</sub>	FeO <sub>4</sub> (H <sub>2</sub> O) <sub>2</sub>	
mean Fe-O bond dist	2.004 Å	2.090 Å	

<sup>a</sup> Data taken from ref 3. <sup>b</sup> This work.

of *x*, and some analytical results are presented in Table I.

The X-powder diffraction patterns were obtained by using either a Guinier camera or a Philips diffractometer. An internal calibration was obtained with KCl.

The Mössbauer effect absorbers were prepared first by grinding selected single crystals of voltaite or its cadmium solution to a fine powder. This fine powder was then mixed with Vaseline to provide random polycrystallite orientation. The concentration of iron was adjusted so that the typical absorbers contained 7–10 mg of <sup>57</sup>Fe/cm<sup>2</sup>. The Mössbauer-effect spectra were obtained either on an Austin Science Associates or a Harwell constant-acceleration spectrometer. Both spectrometers utilized a room-temperature rhodium-matrix source and were calibrated with natural  $\alpha$ -iron foil. The liquid-helium spectra were obtained in cryostats in which the sample was placed directly in the liquid helium. The temperatures of the samples studied below 4.2 K were obtained by measuring the vapor pressure of helium above the liquid. The magnetically perturbed spectra were obtained with either a British Oxygen Corp. superconducting magnet and cryostat, which produced a transverse field, or an Oxford Instruments Corp. superconducting magnet and cryostat, which produced a longitudinal field. In each case, the applied magnetic field was calibrated by measuring the change in the iron foil internal hyperfine field produced by the magnet. The Mössbauer spectra were evaluated by using least-squares minimization programs and the IBM 370/168 computer facilities of the University of Missouri and Harwell. The Mössbauer-effect parameters reported herein have error limits of at least  $\pm 0.02$  mm/s and, in many cases, of  $\pm 0.01$  mm/s. The distribution of the internal hyperfine fields was determined by using a technique developed by Window.<sup>8</sup> The internal fields reported herein are accurate to either ca. 5% or 10 kOe, whichever is largest.

## Results and Discussion

The crystalline structure of voltaite,  $K_2Fe_8Al(SO_4)_{12} \cdot 18H_2O$ , has been very accurately determined by Mereiter.<sup>3</sup> A summary of his results is presented in Table II. Voltaite is cubic and contains two crystallographically distinct sites, which may be occupied by iron. In the first of these sites, labeled M(1) by Mereiter, the iron is coordinated by six oxygen atoms from the sulfate in a slightly trigonally distorted octahedral geometry. There are 32 of these sites per unit cell, and the average iron–oxygen distance of 2.004 Å indicates that this site contains iron(III). In the second, M(2) site, the iron is coordinated by four oxygen atoms from the sulfate and two water molecules in a trans pseudooctahedral coordination geometry. There are 96 of these sites per unit cell. The average iron–oxygen distance is 2.097 Å, and the iron–water distance is 2.075 Å. Mereiter's analysis indicates that the M(2) site is occupied by 16 iron(III) ions and 80 iron(II) ions for an iron(II) to iron(III) ratio of five. His results are most consistent with a zero occupancy of the M(1) site by iron(II), but he could not rule out the possibility of a small number of iron(II) ions

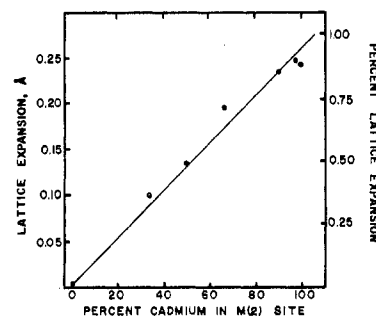


**Figure 1.** Lattice expansion of voltaite as a function of cadmium content relative to a value of 27.249 Å for voltaite.

on the M(1) site. This of course slightly reduces the iron(II) to iron(III) ratio on the M(2) site. These results are also summarized in Table II.

The X-ray powder diffraction results for our sample of voltaite were indexed on the basis of Mereiter's work, and the resulting cubic lattice parameter was only 0.02% less than that reported by Mereiter<sup>3</sup> (Table II). The powder neutron diffraction results<sup>2</sup> indicate no structural phase transition between room temperature and 3 K, but it does show an approximate 0.3% lattice contraction over this temperature range and no indication of any magnetic ordering at temperatures down to 3 K. The X-ray powder diffraction results for the cadmium-containing samples demonstrate that they retained the cubic voltaite structure. Again, these results were indexed to the voltaite structure, and an accurate cubic lattice parameter was refined for each sample. The results indicate the expected increase in unit cell size as the larger cadmium(II) replaces iron(II) in the voltaite. As depicted in Figure 1, the linear increase in the lattice parameter is accompanied by an increase in cadmium in the M(1) site.

It is interesting to note that the amount of cadmium incorporated into voltaite in its various compositions does not necessarily correspond to that expected from the cadmium to iron(II) ratio used in the preparation. It is apparent from an inspection of Table I that at low cadmium concentrations the incorporation of cadmium is actually favored over iron(II). For instance, at a one to one initial ratio, the expected compound would be  $K_2Fe^{II}_{2.5}Cd_{2.5}Fe^{III}_3Al(SO_4)_{12} \cdot 18H_2O$ , whereas the compound that is formed is  $K_2Fe^{II}_{2.1}Cd_{2.9}Fe^{III}_3Al(SO_4)_{12} \cdot 18H_2O$ . At higher initial cadmium concentrations, this enhanced incorporation ceases or is perhaps reversed. The Mössbauer spectral results discussed below indicate that the electronic symmetry at the iron(II) M(2) site increases with increasing cadmium content. Apparently, the presence of the cadmium on the M(2) site slightly changes the local symmetry perhaps by reducing the strain in the Fe–O–S bridging angles, and this improves the total bond energy. This improvement could lead to a higher thermodynamic stability and, hence, to the enhanced incorporation of cadmium. Alternatively, the enhancement could be the result of a higher preference of iron(II) for the mother liquor.

**Mössbauer Spectral Results for Voltaite.** The Mössbauer spectrum of voltaite,  $K_2Fe^{II}_5Fe^{III}_3Al(SO_4)_{12} \cdot 18H_2O$ , obtained at 78 K is illustrated in Figure 2. Very similar results are obtained at 4.2 K (Figure 3). In each case, four lines are clearly resolved. The room-temperature spectrum is similar to that shown in Figure 2 except that there is less resolution of the three lines centered at ca. 0.4 mm/s. The Mössbauer-effect spectral parameters for this compound are recorded in Table III.

As mentioned above, Mereiter's X-ray analysis<sup>3</sup> does not rule out the possibility that a small number of iron(II) ions occupy the M(1) site. It is thus of interest to determine the amount of iron(II) on the M(1) site through the Mössbauer

(8) Window, B. J. *Phys. E* 1971, 4, 401.

Table III. Voltaite Mössbauer-Effect Spectral Parameters<sup>a</sup>

site designatn	x	rel <sup>b</sup> total area	292 K			78 K			4.2 K		
			$\Delta E_Q$	$\delta$	$\Gamma$	$\Delta E_Q$	$\delta$	$\Gamma$	$\Delta E_Q$	$\delta$	$\Gamma$
Fe(II); M(2)	5.00	2.000	1.80	1.27	0.38	2.68	1.42	0.52	2.72	1.42	0.46
	3.10	2.000	1.72	1.21	0.51	2.51	1.42	0.62	2.53	1.42	0.57
	2.10	2.000	1.68	1.20	0.54	2.40	1.39	0.60	2.50	1.46	0.62
	1.05	2.000	1.61	1.19	0.71	2.25	1.48	0.77	2.43	1.46	0.58
	0.53	2.000	1.59	1.17	0.70	2.26	1.42	0.75			
	0.24	2.000	c	c	c	2.49	1.24	0.63			
Fe(III); M(1)	5.00	0.800		0.45	0.40		0.48	0.38		0.47	0.42
	3.10	1.290		0.50	0.44		0.48	0.42		0.49	0.39
	2.10	1.905		0.47	0.48		0.49	0.51		0.50	0.43
	1.05	3.810		0.53	0.45		0.46	0.54		0.49	0.46
	0.53	7.547		0.38	0.55		0.46	0.54			
	0.24	16.667		0.37	0.54		0.47	0.57			
Fe(III); M(2)	0.19	21.052		0.36	0.56		0.46	0.57			
	0	2.000		0.38	0.55		0.43	0.51		0.47	0.50
	5.00	0.400		0.62	0.40		0.77	0.25		0.75	0.28
	3.10	0.645		0.68	0.35		0.76	0.29		0.76	0.28
	2.10	0.952		0.68	0.32		0.76	0.36		0.78	0.31
	1.05	1.905		0.63	0.31		0.76	0.36		0.78	0.32
	0.53	3.774		0.67	0.38		0.76	0.40			
	0.24	8.333		0.67	0.38		0.79	0.44			
	0.19	10.526		0.66	0.40		0.77	0.43			
	0	1.000		0.67	0.42		0.75	0.43		0.77	0.35

<sup>a</sup> All data in mm/s relative to natural  $\alpha$ -iron foil. <sup>b</sup> Constrained to the relative areas given (see text). <sup>c</sup> Component not observed.

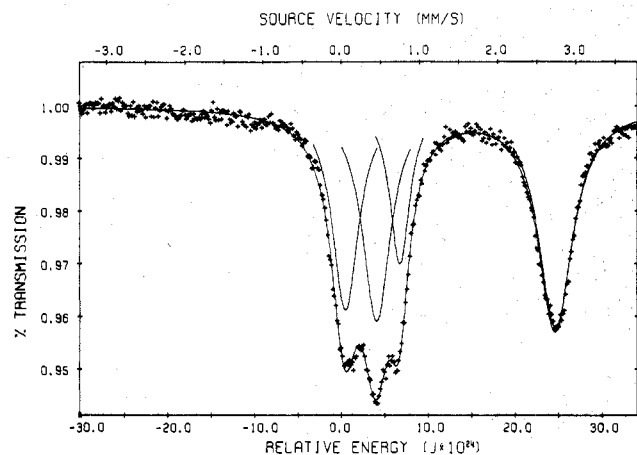


Figure 2. Unconstrained fit to the 78 K Mössbauer-effect spectrum of voltaite.

effect. Hermon et al.<sup>6</sup> in this way concluded that four of the M(1) sites are occupied by iron(II) and that 20 iron(III) ions occupy the M(2) site. Such an analysis<sup>9</sup> is, however, difficult because the iron(II) and iron(III) lines in the spectra obtained by Hermon et al.<sup>6</sup> are poorly resolved and because of the difficult problem of accounting for the potential difference in the recoil-free fraction, i.e., the relative area, for the different crystallographic sites and oxidation states.

We have concluded on the basis of two lines of evidence that voltaite is probably best described by the occupancy factors obtained by Mereiter<sup>3</sup> and listed in Table II. In other words, we find no evidence of any iron(II) on the M(1) site. If in fact iron(II) does occupy the highly symmetric M(1) site, it should exhibit a small quadrupole interaction (probably at most 1.0 mm/s) and an isomer shift of 1.2–1.4 mm/s at 78 K. Under these circumstances, we should see an absorption in the range of 1.2–1.9 mm/s. As illustrated in Figures 2 and 3, no absorption is observed in this velocity range. We estimate from the quality of our data, that we should be able to observe as little as one iron(II) in the M(1) site. Hence, we conclude that

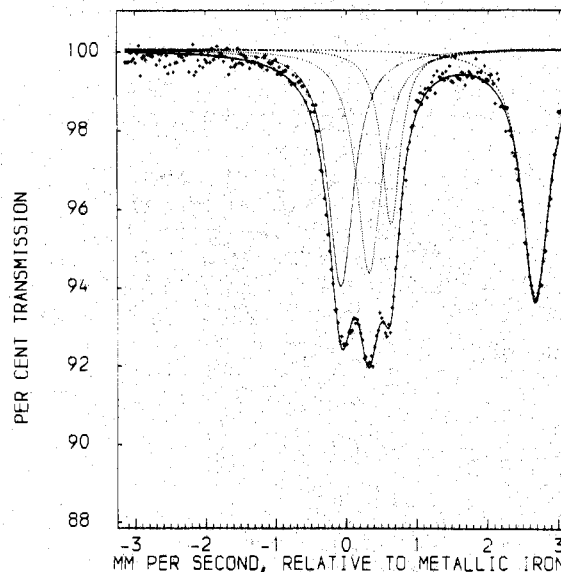
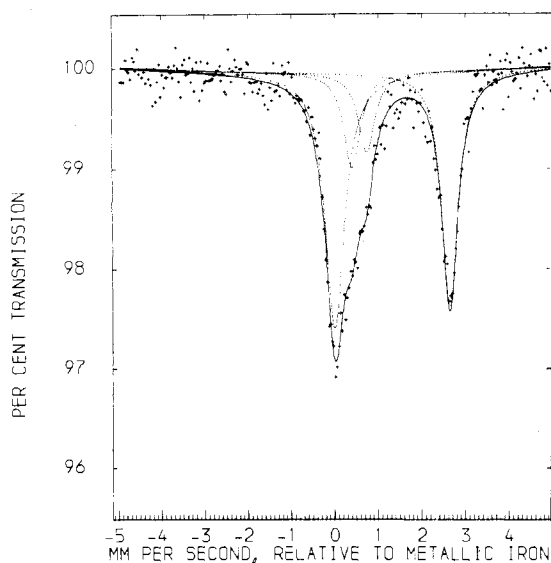


Figure 3. Unconstrained fit to the 4.2 K Mössbauer-effect spectrum of voltaite.

there is at most one, and most likely fewer, iron(II) ions on the M(1) site.

This conclusion is further supported by the relative area of the observed Mössbauer absorption bands. Mereiter's occupancy factors indicate that the ratio of Fe(II),M(2) to Fe(III),M(1) to Fe(III),M(2) should be 80:32:16 or 5:2:1. Because of the low symmetry of the M(2) site, we should expect a large quadrupole interaction for the Fe(II),M(2) component. Alternatively, the quadrupole interaction for the two iron(III) sites should be small. On this basis, we have assigned the first and fourth lines in Figures 3 and 4 to the Fe(II),M(2) ion. The second line is assigned to Fe(III),M(1) and the third line to Fe(III),M(2). This assignment should lead to a relative area for the four lines of 2.5:2:1:2.5 or 1:0.8:0.4:1 if the recoil-free fraction is the same for all three sites. The totally unconstrained fit to the four lines that is illustrated in Figure 2 indicates a ratio of 0.90:1.00:0.40:1.00. If the two lines of the quadrupole doublet are constrained to an equivalent line width and area, the ratio is 1.00:0.87:0.4:1.00. In both instances, the relative area of the

(9) The presence of four iron(II) ions on M(1) (as suggested by Hermon et al.<sup>6</sup>) would require 28 iron(III) ions on M(1) and 20 iron(III) ions on M(2). This would correspond to an Fe(III),M(1) to Fe(III),M(2) ratio of 1.4, a value far below the observed ratio of 2.1–2.5.



**Figure 4.** Unconstrained fit to the 1.3 K Mössbauer-effect spectrum of voltaite.

iron(III) lines is high, and the ratio of the Fe(III),M(1) to Fe(III),M(2) area is higher than the expected value of 2. From this, we conclude that the  $f$  factor is higher for the iron(III) sites than for the iron(II) site. This conclusion is certainly consistent with our expectation of the relative binding of the iron in the three different cases, and it provides additional support for our contention that there is little if any iron(II) on the M(1) site. The appearance of iron(II) on the M(1) site would require a ratio of Fe(III),M(1) to Fe(III),M(2) of less than 2, the opposite of what we observe.

The Mössbauer-effect parameters resulting from the assignments mentioned above are listed in Table III. A cursory examination of Figure 3 might lead to the alternative assignment of lines two and four to the quadrupole split Fe(II),M(2) site. We reject this assignment, because it gives an unreasonably high value of 1.62 mm/s for the isomer shift at 78 K. The same would be true for the room-temperature and 4.2 K results. In addition, it yields inconsistent results for the voltaite cadmium solid-state solution spectra, whereas the first assignment is consistent in all cases.

In order to reduce the number of free parameters in our least-squares fitting procedure, we prefer to use the following constraints. In all cases, the areas and line widths of the two, quadrupole split, iron(II) lines are constrained to be equivalent. In addition, in spite of our previous assertion, we have constrained the relative areas to the occupancy factors derived by Mereiter.<sup>3</sup> These constraints apply to all the parameters reported in Table III in which the constrained relative total areas of each site are listed. We have adopted this procedure, because we need it to facilitate the analysis of the cadmium-containing materials whose reduced iron(II) content produces poorly resolved spectra. In any case, no significant difference exists between the quadrupole interaction and isomer shift values reported in Table III for voltaite ( $x = 5.00$ ) even when the constraints are completely removed. The line widths, and relative areas do, however, change, and the  $\chi^2$  values show a small decrease as a result of the increase in the number of degrees of freedom. Dollase<sup>10</sup> discussed the relationship between the extent of the overlap of adjacent Mössbauer spectral lines and the extent to which the relative areas and line widths of the absorptions may be determined. On the basis of his results, we conclude that inclusion of the constraints, which are based on sample chemical analysis, leads to the best

spectral parameters. It should be noted that for voltaite ( $x = 5.00$ ) at 78 and 4.2 K the resolution of the four observed lines exceeds the criterion of 0.6 $\Gamma$  established by Dollase for adequate resolution without constraints. This is in agreement with our observation that the constrained and unconstrained fits give virtually the same Mössbauer spectral parameters and that the resolution of the four lines is readily visible to the eye (Figures 3 and 4). However, the room-temperature spectrum of voltaite and the spectra of many of the solid-state solutions with cadmium do not meet this criterion, and, hence, the application of the constraints seems reasonable.

The Mössbauer spectral parameters for voltaite (Table III) appear to be very acceptable in view of its known structure. As noted previously,<sup>2</sup> there is no single-valence iron(II) compound that contains the *trans*-Fe(H<sub>2</sub>O)<sub>2</sub>(SO<sub>4</sub>)<sub>4</sub> coordination geometry. Perhaps the best comparison can be made with FeSO<sub>4</sub>·7H<sub>2</sub>O and Fe(ClO<sub>4</sub>)<sub>2</sub>·6H<sub>2</sub>O with their [Fe(OH<sub>2</sub>)<sub>6</sub>]<sup>2+</sup> distorted coordination geometry and with anhydrous FeSO<sub>4</sub> which is a distorted FeO<sub>6</sub> coordination geometry.<sup>11</sup> These three compounds yield room-temperature isomer shift values of 1.26,<sup>11</sup> 1.34,<sup>13</sup> and 1.27 mm/s,<sup>12</sup> which agree well with the values of 1.27 mm/s found for voltaite. Similar excellent agreement is found at lower temperatures. There are larger variations in  $\Delta E_Q$  for these compounds. The respective room-temperature values are 3.24,<sup>11</sup> 1.43,<sup>13</sup> and 2.73 mm/s.<sup>12</sup> In all cases,  $\Delta E_Q$  increases with a decrease in temperature. This range of values and their temperature dependence are not unexpected in view of the predominant valence contribution to the EFG tensor in these distorted octahedral iron(II) complexes.<sup>14,15</sup> The values of  $\Delta E_Q$  for voltaite indicate that the M(2) site in voltaite is apparently less distorted than the iron sites in FeSO<sub>4</sub> and FeSO<sub>4</sub>·7H<sub>2</sub>O and is similar to that found in Fe(ClO<sub>4</sub>)<sub>2</sub>·6H<sub>2</sub>O. An attempt to determine the sign of  $\Delta E_Q$  in an applied field Mössbauer effect experiment failed because overlapping bands arose from the iron(III) present.

We have assigned the Mössbauer-effect absorptions observed at 78 K in voltaite at 0.48 and 0.77 mm/s to the iron(III) ions located on the M(1) and M(2) sites, respectively. We have based this assignment on the relative intensities of the two lines. The line at 0.48 mm/s has approximately twice the area of the 0.77 mm/s absorption. The expected ratio is 2.0, whereas the observed ratio is 2.5 for the totally unconstrained fit and 2.1 for the partially constrained fit. As expected for a high-spin <sup>6</sup>A<sub>1g</sub> iron(III) ion in a close to cubic environment, we observed no quadrupole splitting. The isomer shift values are in excellent agreement with the values obtained in anhydrous monoclinic<sup>16</sup> and rhombohedral<sup>17</sup> iron(III) sulfate, both of which have coordination geometries<sup>18-20</sup> very similar to that of the Fe(III),M(1) site in voltaite. It is surprising that the voltaite M(1) site with its FeO<sub>6</sub> coordination geometry has a larger line width than the M(2) site with its FeO<sub>4</sub>(OH<sub>2</sub>)<sub>2</sub> geometry. Although the difference is not too large, it is found at all temperatures (Table III). We currently have no explanation for this result.

It should be mentioned at this point that our results, presented in Table III, show some distinct differences from those

(10) Dollase, W. A. *Am. Mineral.* **1975**, *60*, 257.

- (11) Greenwood, N. N.; Gibb, T. C. "Mössbauer Spectroscopy"; Chapman and Hall: London, 1971; p 133.
- (12) Grant, R. W.; Wiedersich, H.; Muir, A. H., Jr.; Gonser, U.; Delgass, W. N. *J. Chem. Phys.* **1966**, *45*, 1015.
- (13) Wroblewski, J. T.; Long, G. J., unpublished results.
- (14) Ingalls, R. *Phys. Rev. A* **1964**, *133*, 787.
- (15) Gibb, T. C. *J. Chem. Soc. A* **1968**, 1439.
- (16) Long, G. J.; Longworth, G.; Battle, P.; Cheetham, A. K.; Thundathil, R. V.; Beveridge, D. *Inorg. Chem.* **1979**, *18*, 624.
- (17) Haven, Y.; Nofle, R. E. *J. Chem. Phys.* **1977**, *67*, 2825.
- (18) Moore, P. B.; Araki, T. *Neues Jahrb. Mineral., Abh.* **1974**, *121*, 208.
- (19) Christidis, P. C.; Rentzeperis, P. J. Z. *Kristallogr. Kristallgeom., Kristallphys., Kristallchem.* **1975**, *141*, 233.
- (20) Christidis, P. C.; Rentzeperis, P. J. Z. *Kristallogr. Kristallgeom., Kristallphys., Kristallchem.* **1976**, *144*, 341.

reported by Hermon et al.<sup>6</sup> These differences exist, because we obtained better resolution in our spectra and used different assumptions and procedures in fitting them.

A comparison of voltaite with other mixed-valency iron-containing minerals seems appropriate. One such well-studied mineral is biotite, an iron and magnesium silicate. Structural work<sup>21,22</sup> indicates that this trioctahedral mica contains two different distorted octahedral coordination sites. The average iron-oxygen bond length at each of these sites is essentially the same at 2.11 Å.<sup>21</sup> One of these sites, M(1), contains the *trans*-MO<sub>4</sub>(OH)<sub>2</sub> coordination geometry, whereas the second, M(2), contains the *cis*-MO<sub>4</sub>(OH)<sub>2</sub> geometry.

Many Mössbauer-effect studies of biotite have been conducted, but the results of three<sup>23-25</sup> are sufficient for our purposes. The analysis of the Mössbauer spectra of biotite is complicated by the abundance of overlapping absorption lines for its different site symmetries and oxidation states; consequently a variety of results have been reported.<sup>26</sup> In spite of this difficulty, some general comparisons can be made. The range of the reported<sup>23-25</sup> room-temperature isomer shifts for the divalent iron sites is 1.03–1.13 mm/s, and the range of  $\Delta E_Q$  is 2.10–2.26 mm/s for M(1) and 2.56–2.67 mm/s for M(2). These values for  $\Delta E_Q$  compare well with those of voltaite (Table III), but the isomer shifts are decidedly smaller than those observed in voltaite. The magnitude of the isomer shifts can be related to the percentage of covalent bonding in the predominately ionic iron-oxygen bonds. In general, it is found that the isomer shifts will decrease with an increase in covalency.<sup>28</sup> Hence, the larger isomer shifts in voltaite indicate a smaller covalent contribution to its iron(II) oxygen bonds as compared with biotite. This difference is also reflected in the smaller valence electron delocalization coefficient observed in voltaite, when it is compared with biotite.<sup>2</sup> Unfortunately, no Mössbauer-effect data are available for bilinite or romerite, both of which are mixed-valence iron sulfate minerals.

Hermon et al.<sup>6</sup> after measuring the low-temperature magnetic susceptibility of voltaite reported that voltaite exhibits Curie-Weiss behavior for temperatures above ca. 10 K. At lower temperatures, the inverse susceptibility diverges from linearity toward the temperature axis in a fashion characteristic of a ferrimagnetic material.<sup>6</sup> By assuming two sublattice ferrimagnetic ordering and by using molecular field theory, they estimated the value of the critical ordering temperature (the ferrimagnetic Néel point) as 0.4 K. In order to confirm this low value for the ordering temperature of voltaite, we measured its Mössbauer spectrum at 1.3 K, the lowest temperature available to us. The results are presented in Figure 4. The fit illustrated in this figure was obtained with no constraints in the fitting procedure. The resulting Mössbauer-effect parameters are for the Fe(II),M(2) site  $\Delta E_Q = 2.64$  mm/s,  $\delta = 1.32$  mm/s, and  $\Gamma = 0.54$  and  $0.45$  mm/s, for the Fe(III),M(1) site  $\delta = 0.40$  mm/s and  $\Gamma = 0.45$  mm/s, and for the Fe(III),M(2) site  $\delta = 0.73$  mm/s and  $\Gamma = 0.35$  mm/s. The total area ratio of Fe(II),M(2) to Fe(III),M(1) to Fe(III),M(2) is 5.00:0.90:0.74. It is immediately apparent from this ratio and from a comparison of Figure 3 with Figure

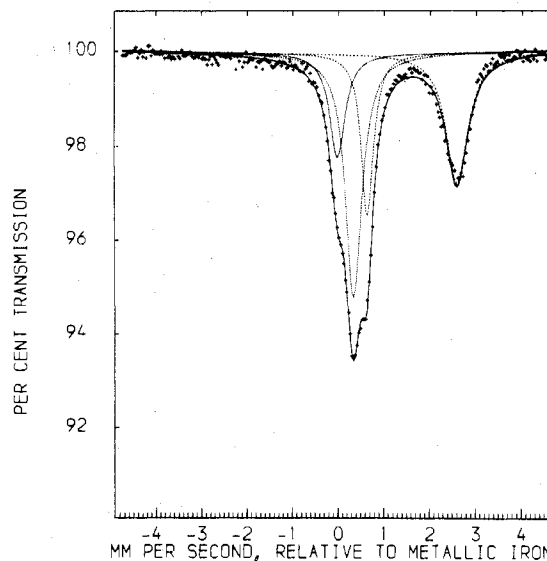


Figure 5. Unconstrained fit to the 4.2 K Mössbauer-effect spectrum of the  $x = 3.10$  voltaite-cadmium solid-state solution.

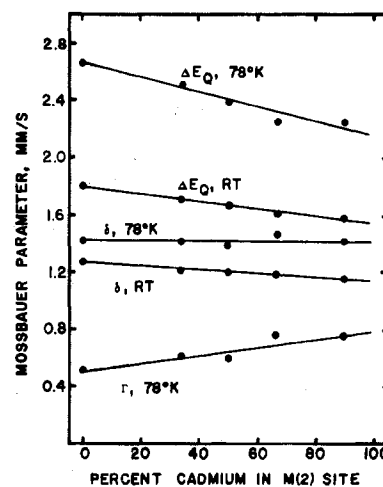


Figure 6. Mössbauer-effect parameters for the Fe(II),M(2) site in the voltaite-cadmium solutions as a function of cadmium content.

4 that the observed intensity of the iron(III) lines decreases relative to the intensity of the iron(II) lines. There does not, however, appear to be a significant change in the total absorption area. The exact reason for this decrease is not completely clear at this time, but it is no doubt related to the onset of magnetic ordering. The decrease may be associated with a decrease in the magnetic relaxation on the iron(III) sites as the ferrimagnetic ordering temperature is approached. This decrease in the relaxation rate could manifest itself as an apparent decrease in the observed intensity of the iron(III) lines relative to the iron(II) lines.<sup>29</sup> Confirmation of this mechanism will probably require Mössbauer studies at even lower temperatures.

#### Mössbauer Spectral Results for Voltaite-Cadmium Solutions.

The Mössbauer-effect spectra of the solid-state solutions of cadmium in voltaite have been measured at several temperatures. In all instances there is an obvious decrease in the intensity of the first and fourth line relative to the intensity observed in voltaite. A typical result, which has been obtained for for the  $x = 3.10$  voltaite-cadmium solution at 4.2 K, is illustrated in Figure 5. The unconstrained fit illustrated in this figure gives the same spectral parameters as those obtained

(21) Donnay, G.; Morimoto, N.; Takeda, H.; Donnay, J. D. H. *Acta Crystallogr.* **1964**, *17*, 1369.

(22) Franzini, M.; Schiaffino, L. Z. *Kristallogr., Kristallgeom., Kristallphys., Kristallchem.* **1964**, *119*, 297.

(23) Annersten, H. *Am. Mineral.* **1974**, *59*, 143.

(24) Bancroft, G. M.; Brown, J. R. *Am. Mineral.* **1975**, *60*, 265.

(25) Goodman, B. A.; Wilson, M. J. *Mineral. Mag.* **1973**, *39*, 448.

(26) This is further complicated by different site notation in different papers. For instance the M(2) site described in ref 23 and 24 is referred to as the M(1) site in ref 25.<sup>27</sup>

(27) Goodman, B. A. *Am. Mineral.* **1976**, *61*, 169.

(28) Goldanskii, V. I.; Makarov, E. F. In "Chemical Applications of Mössbauer Spectroscopy"; Goldanskii, V. I., Herber, R. H., Eds.; Academic Press: New York, 1968; p 1.

(29) Wickman, H. H.; Klein, M. P.; Shirley, D. A. *Phys. Rev.* **1966**, *152*, 345.

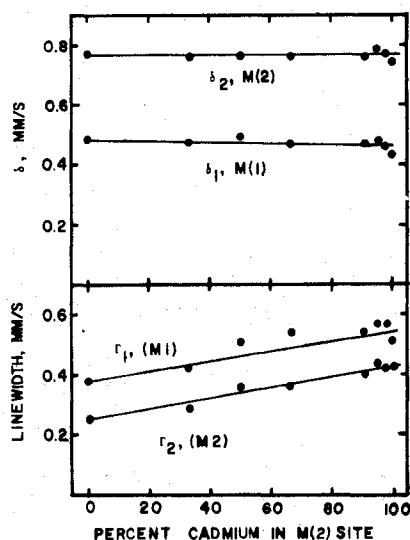


Figure 7. Mössbauer-effect parameters for the Fe(III) sites in the voltaite-cadmium solutions as a function of cadmium content.

when using the constrained fits discussed above. The constrained parameters for all of the solutions are presented in Table III. In all instances, the removal of the fitting constraints leads to only a slight lowering of  $\chi^2$  and to essentially the same parameters as those reported in Table III. For  $x = 0$ , there is no indication of any absorption, which can be attributed to iron(II) (see below).

The results presented in Table III as a function of  $x$  are interesting, because they show how the electronic and structural properties of voltaite are affected by the presence of cadmium on the M(2) site. As mentioned above, X-ray diffraction studies indicate no structural modifications with an increase in cadmium content. There is, however, a linear increase in the cubic lattice parameter with an increase in cadmium (Figure 1). As might be expected, the Mössbauer spectral properties exhibit a regular change as the cadmium content increases. This is illustrated in Figure 6 for the Fe(II),M(2) site and in Figure 7 for the two iron(III) sites. It is apparent from an inspection of these figures that in all instances the isomer shift is independent of the cadmium content. This indicates that the presence of the cadmium has essentially no effect on the covalency of the iron-oxygen bond and that the average iron-oxygen bond distance must be relatively independent of  $x$  even for the M(2) lattice site.

In contrast, the quadrupole interaction for the Fe(II),M(2) site displays a distinct decrease as the cadmium content increases at 78 K and a smaller decrease at room temperature. This decrease in  $\Delta E_Q$  indicates that the electronic symmetry at the iron(II) site increases with an increase in cadmium content. If the iron(II) ion were in an exact octahedral environment, the  $t_{2g}$  orbitals would be degenerate and the valence contribution to the EFG tensor would be zero.<sup>14</sup> Because the lattice contribution is expected to be small, the quadrupole interaction would be close to zero. As the degeneracy of the  $t_{2g}$  orbitals is removed by reducing the octahedral symmetry, a nonspherical crystal field potential is produced for this  $t_{2g}^6 e_g^2$  electronic configuration, and there is a large valence contribution to  $\Delta E_Q$ . The observed quadrupole splitting is created predominately by the rather low symmetry of the *trans*-FeO<sub>4</sub>(H<sub>2</sub>O)<sub>2</sub> coordination geometry and its resulting valence contribution to the EFG tensor. Hence, the presence of cadmium in the M(2) site must increase the electronic symmetry at the remaining M(2) sites occupied by iron(II). It seems unlikely that the observed 11% decrease in  $\Delta E_Q$  with  $x$  could be solely a change in the lattice contribution to the EFG tensor.<sup>14</sup> This improved symmetry at the M(2) site could

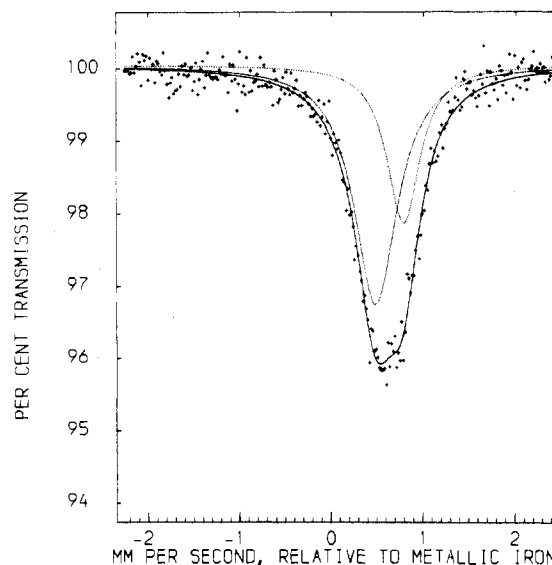


Figure 8. Constrained fit to the 1.3 K Mössbauer-effect spectrum of  $K_2Cd_5Fe^{113}Al(SO_4)_{12} \cdot 18H_2O$ .

result from an improvement in the Fe-O-S bonding angles or other angles at the sulfate groups, which form the extended framework for this crystal structure. As discussed above, this same factor may also be responsible for the enhanced incorporation of the cadmium into the voltaite at low cadmium to iron(II) ratios.

The results presented in Figures 6 and 7 also indicate that the line width for each of the three absorptions increases with an increase in the cadmium content. This increase is probably brought about by the random distribution of the iron(II) and cadmium(II) ions in the M(2) lattice sites. This random distribution produces a small deviation in the cubic symmetry at the iron(III) sites and generates a small quadrupole interaction, which is unresolved in our results and is revealed in a large line width.

**Mössbauer Spectral Results for  $K_2Cd_5Fe^{113}Al(SO_4)_{12} \cdot 18H_2O$ .** The voltaite compound in which cadmium completely replaces the iron(II) on the M(2) site is useful because it allows us to study the material via the Mössbauer effect of the iron(III) sites alone. The Mössbauer-effect spectrum of this compound between room temperature and 4.2 K exhibits a partially resolved two-line spectrum. The spectrum obtained at 1.3 K, as illustrated in Figure 8, is similar but shows less resolution of the two different sites. As a result, the fit illustrated in Figure 8 has been constrained to an area ratio of 2.0 for the Fe(III),M(1) to Fe(III),M(2) sites. The resulting Mössbauer parameters at 1.3 K are  $\delta = 0.48$  mm/s and  $\Gamma = 0.58$  mm/s for the M(1) site and  $\delta = 0.78$  mm/s and  $\Gamma = 0.44$  mm/s for the M(2) site. In the unconstrained fit, the parameters remain essentially the same, but the area ratio decreases to 1.4. Reference to Table III reveals that the isomer shift is essentially the same at 1.3 and 4.2 K, whereas the line widths of the 1.3 K lines are larger than those of 4.2 K. The results obtained at 1.3 K indicate that  $K_2Cd_5Fe^{113}Al(SO_4)_{12} \cdot 18H_2O$  is a paramagnetic material at this temperature, but the increased line widths at 1.3 K indicate that the compound may be very close to its ordering temperature. This would not be surprising in view of the results presented above and the magnetic properties measured by Hermon et al.<sup>6</sup> for voltaite.

In order to learn more about the low-temperature magnetic properties of this compound, we obtained its Mössbauer-effect spectrum in several transverse and longitudinal applied magnetic fields. These results are illustrated in Figures 9 and 11 and recorded in Table IV. It is apparent from Table IV and Figure 9 that the hyperfine field generated by a given applied

Table IV. Applied Field Mössbauer Spectral Parameters for  $K_2Cd_5Fe^{III}_3Al(SO_4)_{12} \cdot 18H_2O$  Obtained at 4.2 K<sup>a</sup>

$H_{app}$ , T	Fe(III),M(1)						Fe(III),M(2)						distribn max			
	$H^b$	$\delta$	QS	$\Gamma$	$\Delta\Gamma^c$	%A	$H^b$	$\delta$	QS	$\Gamma$	$\Delta\Gamma^c$	%A	$I^d$	$\chi^2$	$H, M(1)^b$	$H, M(2)^b$
2, long	207	0.55	+0.04	0.14	1.42	76	72	0.48	+0.07	0.26	1.65	24	0	1.50	212	96
3, trans	337	0.55	+0.05	0.11	1.68	72	103	0.59	+0.01	0.29	1.17	28	4	1.29	339	~110
4.2, long	386	0.59	-0.03	0.11	0.80	62	188	0.43	+0.06	0.30	1.00	38	0	2.72	392	184
6, trans	489	0.58	-0.04	0.14	0.73	61	333	0.52	+0.07	0.31	1.11	39	4	1.42	493	245, 330

<sup>a</sup> Data in mm/s relative to natural  $\alpha$ -iron foil. <sup>b</sup> Internal magnetic hyperfine field in kOe. <sup>c</sup> The incremental line width increase for the outermost magnetic lines. <sup>d</sup> Constrained intensity ratio of line 2 (or 5) to line 3 (or 4).

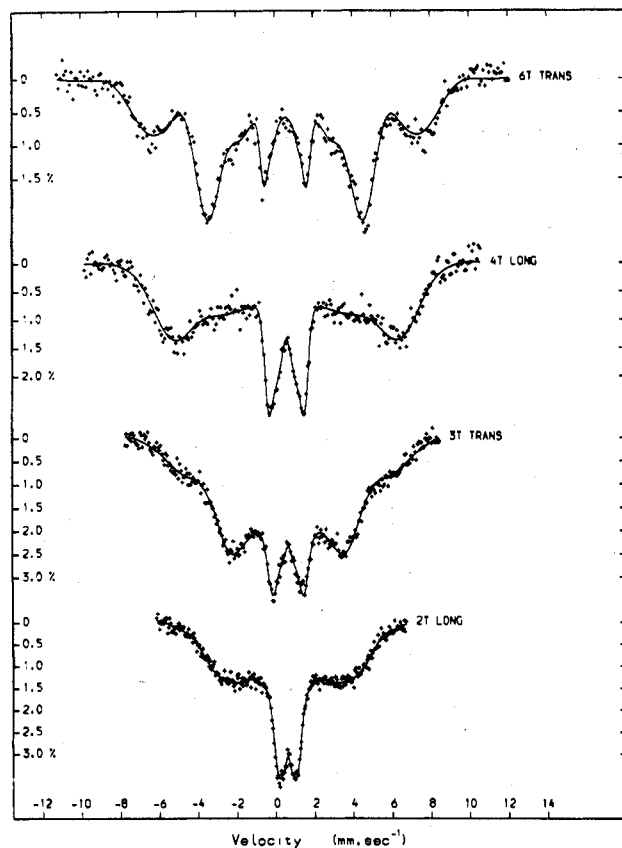


Figure 9. 4.2 K Mössbauer-effect spectra of  $K_2Cd_5Fe^{III}_3Al(SO_4)_{12} \cdot 18H_2O$  obtained in transverse and longitudinal applied magnetic fields of 2–6 T. The fits are discussed in the text.

field is much larger than the applied field. The analysis of the resulting spectra is, however, complicated by the fact that there are two different iron(III) sites in  $K_2Cd_5Fe^{III}_3Al(SO_4)_{12} \cdot 18H_2O$  which have different hyperfine fields. In order to evaluate the resulting, partially resolved magnetic spectra, we used the method developed by Window<sup>8</sup> to determine the distribution of hyperfine fields contained in the spectra. In this method, an approximate line width and the relative intensities of the six hyperfine lines must be specified. In all cases, the calculated distribution yielded a much smaller  $\chi^2$  value, when the intensity ratio was constrained to 3:4:1:1:4:3 for the results obtained in a transverse applied magnetic field— $H_{app}$  normal to the  $\gamma$ -ray propagation direction—and 3:0:1:1:0:3 for the results obtained in a longitudinally applied magnetic field— $H_{app}$  parallel to the  $\gamma$ -ray—than for other ratios. This implies that the hyperfine fields are aligned parallel with the applied field in each case, as would be expected for a paramagnet. However the broad lines observed are inconsistent with rapid relaxation. For the results obtained at 4.2 K and reported in Table IV, the distribution of hyperfine fields produced either two or three resolved peaks with the higher field peak approximately 2 to 3 times the area of the lower field peak or peaks. The width of the observed peaks

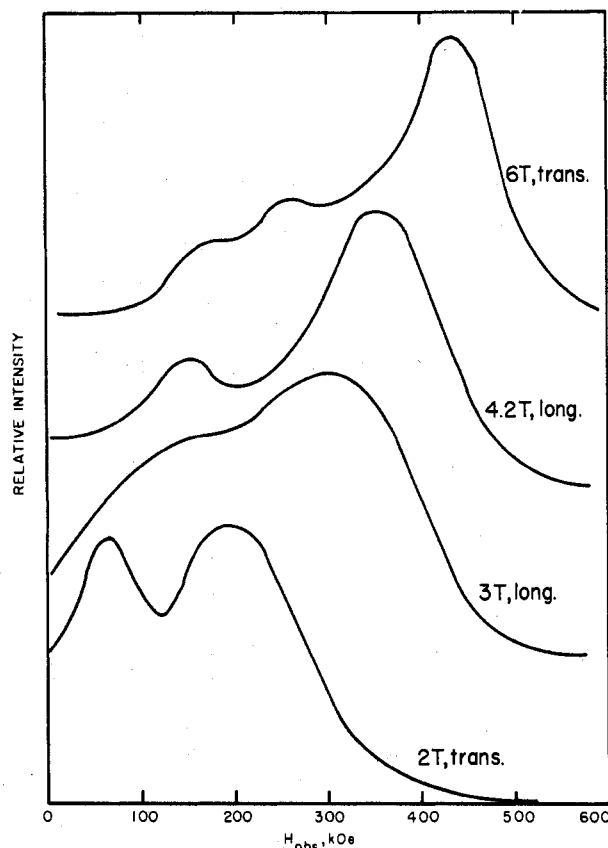
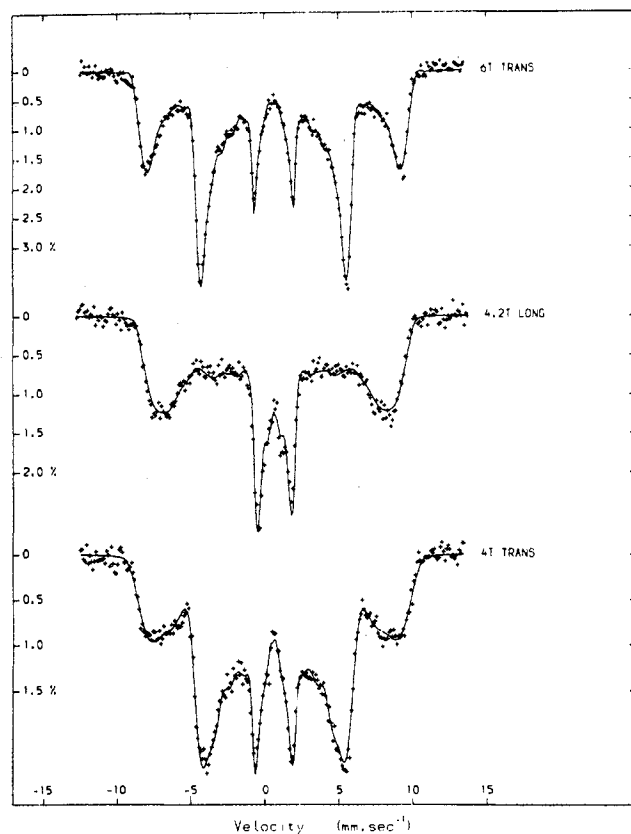


Figure 10. Distribution of the observed hyperfine fields at 4.2 K in  $K_2Cd_5Fe^{III}_3Al(SO_4)_{12} \cdot 18H_2O$  in several transverse and longitudinal applied magnetic fields.

decreased with an increase in the applied field. The indicated maximum values for the hyperfine fields are listed as the distribution maxima in Table IV and the distributions are illustrated in Figure 10. The assignments are based upon the relative site populations (see Table II) and the area under the peaks.

The hyperfine fields obtained from the above analysis were then used to obtain initial parameters for a linear least-squares fitting procedure to further analyze the applied field spectra. The only constraints used for these fits were (1) the restriction to only two magnetic spectra (i.e., 12 lines) and (2) the restriction of the relative areas described above. The Mössbauer-effect parameters resulting from these analyses are included in Table IV and are illustrated by the solid lines in Figure 9. In our fitting procedure, the distribution of hyperfine fields was accounted for by an incremental line width increase,  $\Delta\Gamma$ . When the constraints on the relative areas of the magnetic lines were removed, there was only a small decrease in  $\chi^2$ . This decrease most likely resulted from the increase in the number of degrees of freedom. In determining the internal hyperfine fields listed in this table, we have assumed a negative hyperfine field and, hence, we have added the applied field to the observed hyperfine field.



**Figure 11.** 1.7 K Mössbauer-effect spectra of  $\text{K}_2\text{Cd}_5\text{Fe}^{\text{III}}_3\text{Al}(\text{SO}_4)_{12}\cdot 18\text{H}_2\text{O}$  obtained in several transverse and longitudinal applied magnetic fields. The fits are discussed in the text.

The parameters reported in Table IV are consistent with our analysis of the Mössbauer spectral properties of voltaite. It appears that the applied field Mössbauer results are not sufficiently resolved to reveal the differences in the isomer shift reported in Table III. For both sites, the observed quadrupole shift, QS, is small as one would expect for high-spin iron(III). In addition, the percentage of area of the high-field set of lines assigned to  $\text{Fe}(\text{III}),\text{M}(1)$  is 2 to 3 times that of the low-field lines assigned to  $\text{Fe}(\text{III}),\text{M}(2)$ . The incremental line width,  $\Delta\Gamma$ , decreases with an increase in the applied field. This behavior would be expected if the relaxation rate ( $1/\tau_{\text{flip}}$ ) is close to the precession rate ( $1/\tau_{\text{Lamor}}$ ) because the effect of increasing  $H_{\text{appl}}/T$  is to increase ( $1/\tau_{\text{flip}}$ ) and hence narrow the lines. The relatively low value of ( $1/\tau_{\text{flip}}$ ) could be due to the approach to magnetic ordering expected at about 0.4 K. A plot of the internal hyperfine fields listed in Table IV as a function of applied field indicate that each site exhibits only a very approximate Brillouin behavior<sup>30</sup> and that neither site is saturated at 4.2 K in a 6-T applied field.

The values of the internal hyperfine fields given in Table IV indicate that neither sites are close to saturation at 4.2 K. In order to further increase the  $H/T$  ratio, and in an attempt to saturate the hyperfine field on at least one of the sites, we have also studied  $\text{K}_2\text{Cd}_5\text{Fe}^{\text{III}}_3\text{Al}(\text{SO}_4)_{12}\cdot 18\text{H}_2\text{O}$  at 1.7 K in a 4- and 6-T transverse and a 4.2-T longitudinal applied magnetic field. The resulting spectra are illustrated in Figure 11 and the distribution of the internal hyperfine fields, obtained as discussed above,<sup>8</sup> are illustrated in Figure 12. The main features observed in these distributions are (1) that the most probable internal hyperfine field increases with increasing  $H/T$ , (2) that the width of the largest peak decreases with

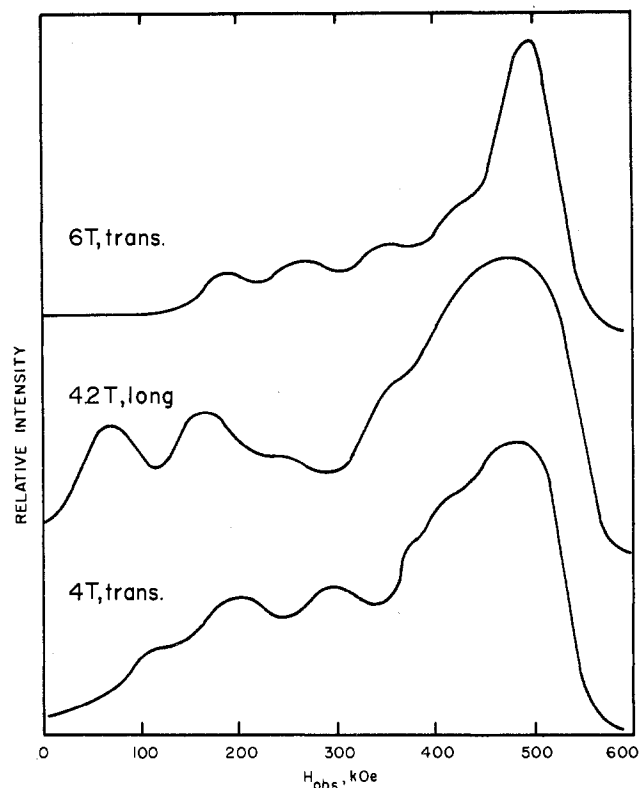


**Figure 12.** Distribution of the observed hyperfine fields at 1.7 K in  $\text{K}_2\text{Cd}_5\text{Fe}^{\text{III}}_3\text{Al}(\text{SO}_4)_{12}\cdot 18\text{H}_2\text{O}$  in several transverse and longitudinal applied magnetic fields.

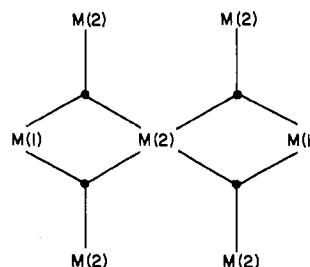


**Figure 13.** Potential exchange coupling pathways through the sulfate groups between an  $\text{M}(2)$  site and its nearest  $\text{M}(1)$  and  $\text{M}(2)$  sites.

increasing  $H/T$ , and (3) that the distribution exhibits either a long "tail" at lower fields or several smaller peaks at lower fields. The most probable values for the internal hyperfine fields are found to be 523, 512, and 555 kOe at applied fields of 4, 4.2, and 6 T, respectively. Hence, the most probable internal hyperfine field, presumably that on the  $\text{Fe}(\text{III}),\text{M}(1)$  site, is saturated at the value of ca. 550 kOe expected for a high-spin iron(III) complex.<sup>31</sup> However, the field on the second, presumably  $\text{Fe}(\text{III}),\text{M}(2)$  site is no longer represented by a unique internal field. Although the small individual peaks found at the lower fields (see Figure 12) may not be significant, the overall broad tail found at lower fields is real. In addition, we have not been able to model the 1.7 K spectra illustrated in Figure 11 with 12 lines resulting from two unique internal hyperfine fields. We believe that this tail represents a distribution of fields present on the  $\text{Fe}(\text{III}),\text{M}(2)$  site. The poorer resolution of the 4.2 K spectra (Figure 9) may conceal this distribution at the higher temperature.

The distribution of internal hyperfine fields in  $\text{K}_2\text{Cd}_5\text{Fe}^{\text{III}}_3\text{Al}(\text{SO}_4)_{12}\cdot 18\text{H}_2\text{O}$  on the  $\text{Fe}(\text{III}),\text{M}(2)$  site may be ex-

(30) Zeiger, H. J.; Pratt, G. W. "Magnetic Interactions in Solids"; Oxford University Press: Oxford, England, 1973; p 91.

(31) Johnson, C. E. In "Hyperfine Interactions in Excited Nuclei"; Goldring, G., Kalish, R., Eds.; Gordon and Breach: New York, 1971; p 803.



plained in the following way. The failure of the lines due to the Fe(III),M(2) to narrow as  $H_{\text{app}}/T$  is increased suggests an additional source of broadening for these sites apart from relaxation broadening. This could be due to the presence of a range of hyperfine fields due to chemical disorder at the M(2) sites. As is discussed below and illustrated in Figure 13, each M(2) ion has four nearest neighbor M(2) sites which are occupied randomly by either Cd(II) or Fe(III). This random distribution could introduce local structural and magnetic disorder leading to a range of saturation fields. This disorder is consistent with the observed X-ray properties for voltaite.<sup>3</sup>

The different behavior of the internal hyperfine field on the two sites may be understood on the basis of the structure of  $K_2Cd_5Fe^{III}_3Al(SO_4)_{12} \cdot 18H_2O$ . The magnitude of the internal hyperfine field on a specific lattice site depends upon the contribution of the isotropic contact interaction arising from the polarization of the s-electron density by the 3d electrons, the contribution of the anisotropic noncontact interaction resulting from the 3d electron orbital moments, and the contribution of the anisotropic noncontact dipolar field of the 3d electron spin.<sup>32</sup> The latter two contributions are expected to be negligible for high-spin iron(III), and hence the first contribution must be primarily responsible for the differences in the magnitude of  $H_{\text{int}}$  for the two different iron(III) sites in this compound. The magnitude of this contribution is known to depend upon the covalency of the iron bonding, and covalency differences are believed to be responsible for the variation in  $H_{\text{int}}$  observed in a variety of high-spin iron(III) compounds.<sup>33</sup> In general, increasing covalency reduces  $H_{\text{int}}$  and increases the isomer shift (see above discussion). A comparison of the data for  $K_2Cd_5Fe^{III}_3Al(SO_4)_{12} \cdot 18H_2O$  presented in Tables III and IV indicates that at 4.2 K the Fe(III),M(2) site has a smaller  $H_{\text{int}}$  and a higher isomer shift than the M(1) site. This indicates that the covalency of the M(2) would be higher than that of the M(1) site. This conclusion is consistent with the

higher covalency expected for the  $FeO_4(H_2O)_2$  coordination sphere of the M(2) site when compared with the  $FeO_6$  coordination sphere of the M(1) site. The postulated range of hyperfine fields at the M(2) sites could be due to differing covalency contributions.

The magnetic susceptibility results of Hermon et al.<sup>6</sup> indicate that  $Tl_2CdFe^{III}_3Al(SO_4)_{12} \cdot 18H_2O$  exhibits Curie-Weiss behavior down to ca. 3 K with a  $\theta$  value of -6 K. Their lowest temperature data reveal a small deviation of the inverse susceptibility toward the temperature axis in a manner similar to that found in voltaite.<sup>6</sup> This behavior is consistent with ferrimagnetic ordering (at a very low critical ordering temperature) of the spins on the two crystallographically different lattice sites. At these temperatures the antiparallel alignment of the spins on the M(1) and M(2) lattice sites would most likely result from a very weak antiparallel superexchange interaction via the sulfate groups that bridge the two lattice sites. As illustrated in Figure 13, a specific Fe(III),M(2) ion is linked to two nearest neighbor Fe(III),M(1) sites via four Fe-O-S-O-Fe pathways. Four similar pathways link the Fe(III),M(2) ion to four other nearest neighbor M(2) sites. It should be noted, however, that each of these nearest neighbor M(2) sites has only a 16.75% chance of containing an iron(III) ion, whereas both of the M(1) sites are occupied 100% by iron(III). As a result, we expect the interaction between M(2) and M(1) to predominate. The difference in magnitude of the internal hyperfine fields on the two sublattices would certainly be consistent with the ferrimagnetic interaction indicated in the magnetic susceptibility studies.<sup>6</sup>

**Acknowledgment.** It is a pleasure to acknowledge the assistance and the helpful discussions that we have had with Drs. B. W. Dale, T. E. Cranshaw, C. E. Johnson, and M. J. Townsend and Messrs. B. Laundy and L. Becker during the course of this work. We thank the Science Research Council for a Research Studentship for D.B. and the National Science Foundation for the financial assistance provided through Grant No. CHE-75-20417.

**Registry No.** Voltaite, 51747-83-2;  $K_2Fe^{II}_5Fe^{III}_3Al(SO_4)_{12} \cdot 18H_2O$ , 72638-81-4; cadmium voltaite, 72638-82-5;  $K_2Cd_5Fe_3^{III}Al(SO_4)_{12} \cdot 18H_2O$ , 72638-83-6.

(32) Chappert, J. *J. Phys. (Paris), Colloq.* 1974, 35, 71.

(33) Greenwood, N. N.; Gibb, T. C. "Mössbauer Spectroscopy"; Chapman and Hall: London, 1971; p 151.

Contribution from the Research Institute for Engineering Sciences and Department of Chemical Engineering and from the Department of Chemistry, Wayne State University, Detroit, Michigan 48202

## Measurement of Boron Trihalide Electron Affinities: Correlation with Boron-Nitrogen Adduct Strengths

ERHARD W. ROTHE,\* B. P. MATHUR, and GENE P. RECK

Received September 18, 1979

The adiabatic electron affinities of several boron trihalides have been measured from the determination of threshold kinetic energies for the reaction  $Cs + BX_3 \rightarrow Cs^+ + BX_3^-$ . A crossed-molecular-beam apparatus was used. The electron affinities are <0.0, 0.33, 0.69, 0.94, and 0.82 eV for  $BF_3$ ,  $BCl_3$ ,  $BCl_2Br$ ,  $BClBr_2$ , and  $BBr_3$ , respectively, with an error estimate of about  $\pm 0.2$  eV. These electron affinities are used to obtain B-N bond energies for adducts of boron trihalides with  $Me_3N$  by using an ionic energy cycle. Values are compared to direct measurements and to those estimated from NMR shift measurements.

### Introduction

Boron trihalide-amine adducts are classic examples of donor-acceptor bond behavior and illustrate an intriguing model of chemical bonding.<sup>1-4</sup> One step in the study of these adducts

is the determination of the relevant properties of the boron trihalides  $BX_2Y$ , where X may be the same as or different from

- (1) P. Cassoux, R. L. Kuczkowski, and A. Serafini, *Inorg. Chem.*, **16**, 3005 (1977).
- (2) P. H. Clippard, J. C. Hanson, and R. C. Taylor, *J. Cryst. Mol. Struct.*, **1**, 369 (1971).
- (3) P. M. Kuznesof and R. L. Kuczkowski, *Inorg. Chem.*, **17**, 2308 (1978).

\* To whom correspondence should be addressed at the Department of Chemical Engineering.